Non-Fermi-liquid behaviour in the weak-coupling approach to correlated fermions

1995 J. Phys.: Condens. Matter 7 7969

(http://iopscience.iop.org/0953-8984/7/41/006)

J. Phys.: Condens. Matter 7 (1995) 7969–7979. Printed in the UK

Non-Fermi-liquid behaviour in the weak-coupling approach to correlated fermions

G Schliecker†, K-D Schotte†, B Horvatić‡ and V Zlatić‡

† Institut für Theoretische Physik, Freie Universität Berlin, Arnimallee 14, D-14195 Berlin, Germany

‡ Institute of Physics, University of Zagreb, PO Box 304, HR-41001 Zagreb, Croatia

Received 12 May 1995, in final form 11 July 1995

Abstract. It has become easy to calculate numerically self-energy corrections in second-order perturbation theory. In order to find out its capabilities and limitations, we analyse the weak-coupling approach for a system of one-dimensional correlated fermions. We compare the self-energy contributions due to different scattering processes of left- and right-moving particles which can be treated analytically. We find that for Tomonaga–Luttinger processes second-order perturbation theory gives reliable results and show how deviations from Fermi-liquid behaviour and the separation of spin- and charge-density excitations can be detected from the numerical data. Choosing the Hubbard model as a typical example we present numerical results for the self-energy and the spectral density. Special attention is paid to the case without particle–hole symmetry. The insulating behaviour at half filling is outside the scope of the weak-coupling method applied.

1. Introduction

One of the main problems for electronic band structures is the understanding of correlation effects. For ordinary metals Fermi-liquid behaviour seems to be a correct description, which means that only the appearance of the Landau terms signals that a metal is not a system of non-interacting or free electrons.

However, for a hypothetical one-dimensional model the free-electron description is invalid, a fermion system has no sharp Fermi surface and behaves as a Luttinger liquid if interaction is taken into account [1, 2]. At present, it is not known if such a deviation from a Fermi liquid also occurs in two-dimensional metals. There are arguments for and against [3, 4, 5] and this is not of only academic interest since the copper oxide layers of high-temperature superconductors are realizations of such two-dimensional metals.

The question we want to study is how perturbation theory can be used to find deviations from Fermi-liquid behaviour. Since it may be hard to extract information even in second order for such systems by analytic means we have analysed the perturbation expansion numerically instead. In the two-dimensional case such a study has been made by Rhodes and Jacobs [6]. In the one-dimensional case analytic and numeric methods are both available and almost everything is known from the Bethe *ansatz* technique or bosonization of the fermionic states. We want to investigate the perturbation approach for the one-dimensional Hubbard model in order to find out its capabilities and its limitations.

The Hubbard model was chosen since it is one of the simplest models with interacting fermions. Nevertheless, all typical scattering processes investigated separately in the theory

0953-8984/95/417969+11$19.50

of the one-dimensional Fermi gas model are included. The Hamiltonian for its one-dimensional version is defined as,

$$H = -\frac{1}{2}\sum_{i,\sigma}\left(c^{+}_{i,\sigma}c_{i+1,\sigma} + c^{+}_{i+1,\sigma}c_{i,\sigma}\right) - \mu\sum_{i,\sigma}c^{+}_{i,\sigma}c_{i,\sigma} + H_U \tag{1}$$

where the first term contains the nearest-neighbour hopping of fermions of spin σ between the sites i and $i+1$. The chemical potential is denoted as μ and H_U describes the on-site interaction between particles of the opposite spin. With the mean-field contributions subtracted it is

$$H_U = U\sum_{i}(n_{i\uparrow} - \langle n_{i\uparrow}\rangle)(n_{i\downarrow} - \langle n_{i\downarrow}\rangle) \tag{2}$$

where $\langle n_{i\sigma}\rangle$ is the mean-field average of the electron density for the site i and the spin label $\sigma = \downarrow, \uparrow$. In the case of half filling or $\langle n_{i\sigma}\rangle = 1/2$ the chemical potential is zero ($\mu = 0$).

The one-dimensional Hubbard model has been solved exactly by Lieb and Wu [7] using the Bethe *ansatz* method. For the half-filled band or the particle–hole symmetrical case there is a gap in the density of states. Away from the symmetric case there is no gap and the one-dimensional Hubbard model behaves like a Tomonaga–Luttinger model [1], for which the correlation functions exhibit a power-law behaviour. The momentum distribution n_p for the momenta p and the density of states $\rho(\omega)$ as a function of frequency ω have the same power-law dependence for the arguments $p - p_f$ or ω as long as they are small. This is the typical property of a Luttinger liquid. The critical exponents and their dependence on band filling n and coupling constant U have been determined recently [8–12].

The standard perturbative approach [13] we want to analyse here expands the self-energy in orders of the coupling constant U. The self-energy Σ and the single-particle propagator G are connected by Dyson's equation:

$$G_p(\omega + \mathrm{i}\delta) = \frac{1}{\omega + \mathrm{i}\delta - \xi_p - \Sigma_p(\omega + \mathrm{i}\delta)} \tag{3}$$

where the kinetic energy is given by $\xi_p = -\cos p - \mu$. The corresponding spectral density is defined as

$$\rho(\omega) = \frac{-1}{\pi}\int_{-\pi}^{\pi}\frac{\mathrm{d}p}{2\pi}\,\mathrm{Im}G_p(\omega + \mathrm{i}\delta). \tag{4}$$

In order to detect deviations from Fermi-liquid behaviour it is necessary to calculate Σ beyond the mean-field approximation linear in U.

The analysis is restricted to second order in U. The starting point is classifying contributions from left- and right-moving particles. This technique is common for the investigation of the one-dimensional Fermi gas model [1] and has also become applicable recently to a two-dimensional system of interacting fermions with a square Fermi surface [3].

In linearizing the cosine dispersion of the Hubbard model analytic results can be obtained for the self-energy. Making use of the classification scheme mentioned above we reduce the self-energy in second order to two different contributions. In this way we show in section 2 that the insulating behaviour at half filling—due to interaction processes with large momentum transfer—is not visible in second order. Contributions which should generate a gap are indistinguishable from contributions which would not. Comparing the numerical result for the Hubbard model with the analytic results, we show that the agreement is very good and that the numerical procedure based on the fast Fourier algorithm [14] is stable and reliable.

The spectral density discussed in section 3 can only be calculated numerically. In special cases, in order to obtain a better understanding, we derive analytic expressions of the Green's function. We discuss the logarithmic corrections connected to the linear behaviour of $\mathrm{Im}\Sigma(\omega)$ for small ω. They reflect the known power-law behaviour of the density of states: $\rho(\omega) \propto |\omega|^{\alpha}$. The pole structure of the self-energy, already found and discussed in [4], gives the splitting in charge- and spin-density excitations.

Perturbation theory does not automatically respect Luttinger's theorem [15] about the constancy of the particle number. By renormalizing the real part of the self-energy we show numerically in the density of states curves that this must be done properly.

2. Self-energy in second order

The retarded self-energy in second order is given by

$$\Sigma_p^{(2)}(\omega^+) = \frac{U^2}{4\pi^2}\int_{-\pi}^{\pi}\int_{-\pi}^{\pi} \mathrm{d}q_1\,\mathrm{d}q_2\,\frac{F(\xi_{q_1},\,\xi_{q_2},\,\xi_{q_1+q_2-p})}{\omega^+ - \xi_{q_1} - \xi_{q_2} + \xi_{q_1+q_2-p}} \tag{5}$$

where $F(\xi_1, \xi_2, \xi_3)$ is the product of Fermi functions $f(\xi) = [1 + \exp(\beta\xi)]^{-1}$:

$$F(\xi_1, \xi_2, \xi_3) = f(\xi_1)f(\xi_2)(1 - f(\xi_3)) + (1 - f(\xi_1))\,(1 - f(\xi_2))\,f(\xi_3) \tag{6}$$

with $\omega^+ = \omega + \mathrm{i}0$. The kinetic energy $\xi_p = -\cos p - \mu$ also contains the chemical potential μ. For numerical calculations it is much more convenient to start from a time- and position-dependent self-energy $\Sigma_R^{(2)}(t)$ and to use the 'fast Fourier' technique to get $\Sigma_p^{(2)}(\omega)$ [14, 16, 17]. However, in order to test the validity of the numerical calculations and to have a better understanding of the results it is necessary to have some analytical results as well. For small $|\omega|$ and $|\mu|$ and momenta close to the Fermi points the self-energy can be evaluated using (5).

2.1. Classification of interaction processes

The restriction to these small parameters means that classifying contributions of right-moving ($\partial\xi_p/\partial p > 0$) and left-moving ($\partial\xi_p/\partial p < 0$) particles makes sense. This means that instead of a single second-order self-energy diagram one has eight. In figure 1, following the traditional discussion, we name them Σ^B and S^B for 'backscattering', Σ^L and S^L for 'Luttinger', Σ^U and S^U for 'Umklapp' and Σ^T and S^T for 'Tomonaga'. They come in pairs since one diagram can be obtained from the other by permuting right and left lines.

In the Hubbard model, where all coupling constants are chosen equal, the backscattering and the Luttinger contributions to the second-order self-energy are found to be equal, i. e.,

$$\Sigma_p^B(\omega^+) = \Sigma_p^L(\omega^+) \qquad S_p^B(\omega^+) = S_p^L(\omega^+). \tag{7}$$

Since the unperturbed Green's functions are even functions of momentum, it is easy to see that a self-energy diagram remains unchanged if one interchanges two-particle lines (those with arrows to the right in figure 1). This way one gets relation (7), which reduces the number of diagrams to six. It also indicates a defect of the approximation: following the renormalization group treatment of the one-dimensional Fermi gas model [1], in the Hubbard model with attractive interaction ($U < 0$) the density of states opens a gap due to backscattering processes. Luttinger processes, however, yield the typical power-law behaviour mentioned above. In the repulsive case ($U > 0$), which we are going to analyse here, the backscattering processes just reduce the critical exponents. Since the self-energies add—see further down equation (9)—the second-order approximation yields an exponent which is too large.

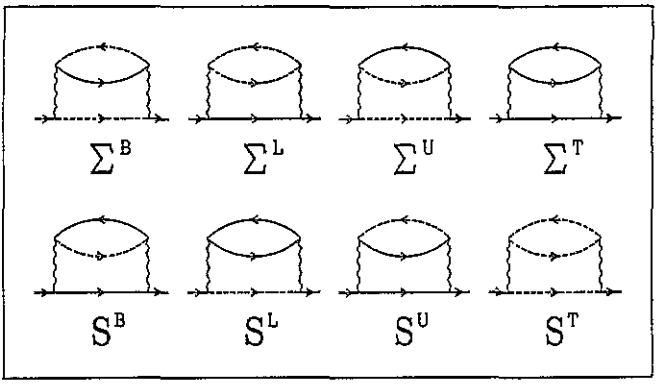

Figure 1. Contributions to $\Sigma_p^{(2)}(\omega)$ with $p > 0$ for the one-dimensional Hubbard model. Solid and dashed lines correspond to right- and left-moving particles, respectively.

Actually, only the Σ terms have to be considered, the S terms being negligible for small $|\omega|$, $|\mu|$ and momenta close to the Fermi points. Since we want the self-energy for small frequencies, only particles with small excitation energies and therefore momenta $\approx p_f$ for right-moving particles and $\approx -p_f$ for left-moving particles give large contributions. Otherwise the denominator in expression (5) would never become small. Adding these internal momenta—forgetting the small deviation from the Fermi points—we obtain the Fermi momentum for the Tomonaga, Luttinger and backscattering diagrams, which is positive for the upper diagrams and negative for the lower ones in figure 1. For the Umklapp diagram, Σ^U (S^U), the momenta add up to $-3p_f$ ($+3p_f$). Since an Umklapp momentum can be added, this is close to p_f ($-p_f$) for small chemical potentials or small deviations from half filling of the band, where $p_f \simeq \pi/2$.

By definition, the sum of the internal momenta just gives p. Thus, for a momentum p close to the Fermi point p_f, the lower diagrams can be neglected, and the self-energy *reduces to the sum of only four diagrams, two of them being identical.*

As we shall see, we just need to make calculations for two of them. To that end, consider what happens if we permute a particle–hole pair, that is, if we turn Σ^L into Σ^U. For small excitation energies and the nearly half-filled band, the particle to hole conversion can be done by reflecting the momentum around the nearest Fermi point, which in fact changes the sign of the energy. Keeping in mind that mainly small excitation energies contribute to the diagrams we get, after some manipulations (see figure 2),

$$\Sigma_p^U(\omega^+) \simeq \Sigma_{p+4p_f}^L(\omega^+). \tag{8}$$

This relation is exact for the half-filled band where $p_f = \pi/2$. For repulsive interaction the Umklapp term, or more precisely the term in the Hamiltonian which generates it, is responsible for the opening of a gap in the half-filled case [1, 19]. However, in equation (8) just an extra $4p_F$ appears as a misfit between Umklapp process and Fermi surface effects, which disables the generation of a gap.

Putting all the contributions together, we have in second order for the self-energy of the Hubbard model

$$\begin{aligned}\Sigma_p^{(2)}(\omega^+) &= 2\Sigma_p^L(\omega^+) + \Sigma_p^U(\omega^+) + \Sigma_p^T(\omega^+) + \text{the } S \text{ terms} \\ &\simeq \Sigma_p^T(\omega^+) + 2\,\Sigma_p^L(\omega^+) + \Sigma_{p+4p_f}^L(\omega^+).\end{aligned} \tag{9}$$

What remains to be done are the calculations of Σ^T and Σ^L. In order to proceed, one

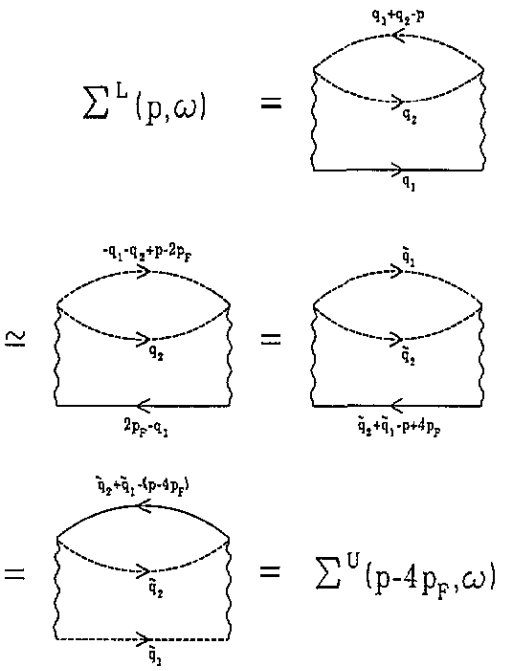

Figure 2. Transformation from Σ^L to Σ^U.

linearizes the cosine dispersion around the Fermi momenta $\pm p_f$, $p_f = \pi/2 + \mu$:

$$\xi_p \simeq v_f|p| - p_f \qquad -\pi < p \leqslant \pi \tag{10}$$

and continued periodically. We restrict our analysis to the nearly half-filled case ($|\mu| \ll 1$), where deviations from the Fermi velocity $v_f = 1$ can be neglected. This approximation gives useful results as long as momenta, frequencies and temperatures are small.

2.2. *Tomonaga and Luttinger contributions*

The Tomonaga self-energy can be evaluated most easily, since all scattering particles move in the same direction. Thus, we just have to integrate the Fermi functions. For the right-moving particles ($p > 0$), we have:

$$\Sigma_p^T(\omega^+) = \frac{U^2}{4\pi^2}\int_0^\pi\int_0^\pi \mathrm{d}q_1\,\mathrm{d}q_2\,\frac{F(q_1-p_F, q_2-p_F, q_1+q_2-p-p_F)}{\omega^+ - \xi_p}. \tag{11}$$

At $T = 0$ the Fermi functions just fix the integration region and we get in accordance with [4]

$$\Sigma_p^T(\omega^+) = \frac{U^2}{8\pi^2}\,\frac{\xi_p^2}{\omega^+ - \xi_p} \tag{12}$$

for small $|\xi_p|$ and $|\omega|$. The integral over the Fermi functions can be done by elementary means, even for $T \neq 0$ if $k_BT \ll 1$. A simple pole in the self-energy yields a splitting into two bands, their separation depending on the strength of the pole. For the Hubbard model in infinite dimensions there is no momentum dependence and the appearance of a $1/\omega$ term in the self-energy signals a Mott–Hubbard gap [20]. Here, however, the pole structure is due to Tomonaga processes, which cannot open a gap. This can also be seen in expression

(12), which vanishes at the Fermi momenta. The resulting Green's function can be written as

$$G_p^T(\omega^+) = \frac{1}{\omega^+ - \xi_p - \Sigma_p^T(\omega^+)} = \frac{1}{2}\left(\frac{1}{\omega^+ - v_-\xi_p} + \frac{1}{\omega^+ - v_+\xi_p}\right) \tag{13}$$

with the renormalized Fermi velocities

$$v_\pm = 1 \pm \frac{1}{\sqrt{2}}\frac{U}{2\pi}. \tag{14}$$

The new excitation energies correspond to the spin- and charge-density excitations in the weak-coupling limit [1]. Thus, expression (13) can be interpreted as a pole approximation of the exact spectral function, which has square-root singularities at $\omega = (1 \pm U/2\pi)\xi_p$ [21].

In order to get the full information for the Hubbard model we also need Σ^L. The evaluation of this diagram can be done by elementary means—in the low-temperature limit. The resulting expression is complicated, but for $T = 0$, $|\mu|$, $|\xi_p|$, $|\omega| \ll 1$ it simplifies to

$$\Sigma_p^L(\omega^+) = u\,(\omega^+ - \xi_p)\ln\left(\frac{\xi_p^2 - \omega^{+2}}{\pi^2}\right) \tag{15}$$

with $u = U^2/(4\pi)^2$.

Due to the logarithm in expression (15), the properties of the corresponding spectral function are now characterized by a branch cut instead of poles. For couplings that are not too large we have

$$-\frac{1}{\pi}\,\mathrm{Im}G_p^L(\omega^+) \simeq u\frac{\Theta(|\omega| - |\xi_p|)}{(\omega - \xi_p)\left\{1 - u\ln\left|(\xi_p^2 - \omega^2)/\pi^2\right|\right\}^2} \tag{16}$$

which can be interpreted as a logarithmic correction of the power-law behaviour in the exact spectral function of the Luttinger model [21],

$$\lambda(x, u) = \frac{1}{1 - 2u\,\ln|x|} \simeq |x|^{2u} \qquad u \ll 1. \tag{17}$$

Following Luttinger [18], it is not too difficult to show that the momentum distribution function n_p in second-order perturbation theory is given by

$$n_p^L = \frac{1}{2} - \frac{1}{2}\,\lambda\left(\frac{\xi_p}{\pi}, u\right). \tag{18}$$

Similarly one obtains for the density of states for the Luttinger contribution:

$$\rho^L(\omega) = \frac{1}{\pi}\,\lambda\left(\frac{\omega}{\pi}, u\right). \tag{19}$$

For both functions, n_p^L and $\rho^L(\omega)$, the expected power-law behaviour is approximated by relation (17).

The decrease of weight in the density of states (19) for small ω can also be understood by a different argumentation. Neglecting the contribution of $\mathrm{Im}\Sigma$, an infinite slope of $\mathrm{Re}\Sigma$ with respect to ω yields a decrease of weight in the spectral function. This effect becomes largest for frequencies close to the excitation energies. The new excitation energies for $\mathrm{Re}\Sigma^L$ are found to be at $\omega = \xi_p$, the divergences of $\partial\mathrm{Re}\Sigma/\partial\omega$ at $\omega = \pm\xi_p$. Thus the decrease of weight in the density of states can be expected to be largest for $\omega \approx 0$.

2.3. Comparison to the numerical result

Combining the results of the last sections in making use of the equations (9), (12) and (15), the analytical result for $\mathrm{Im}\Sigma$ in second-order perturbation theory can be written as

$$\frac{1}{u\pi}\,\mathrm{Im}\,\Sigma_p^{(2)}(\omega^+) = -2\xi_p^2\delta(\omega-\xi_p) \\ -2\,|\omega-\xi_p|\;\Theta\big(|\omega|-|\xi_p|\big) - |\omega-\xi_{p+4p_F}|\;\Theta\big(|\omega|-|\xi_{p+4p_F}|\big) \tag{20}$$

which is valid for $|\omega|, |\xi_p|, |\mu| \ll 1$ and zero temperature. In figure 3, this expression is compared to the numerical result for $\mathrm{Im}\Sigma$ of the Hubbard model. Although the Hubbard model has a cosine dispersion instead of the linear dispersion used in the analytic calculations, both curves agree excellently even for $|\omega| \approx 0.5$. Not only the linearity due to Luttinger processes, but also the weighted δ-function peaks are reproduced by the numerical result. Since both properties can be easily detected from numerical data, the second-order approximation combined with the fast Fourier technique form a reliable tool for a detection of Luttinger-liquid behaviour.

At first sight, the analytical expression for the real part of Σ gives just a fair fit (compare figure 4). The main difference, however, is linear in $\omega - \xi_p$. The missing correction would just yield a renormalization of the the coupling constant and the Green's function, since

$$G_p^{(2)}(\omega^+) = \frac{1}{\omega^+ - \xi_p - \Sigma_p^{(2)}(\omega^+) + \text{constant} \times (\omega^+ - \xi_p)} \\ = \frac{1}{1+\text{constant}}\;\frac{1}{\omega^+ - \xi_p - (1/(1+\text{constant}))\,\Sigma_p^{(2)}(\omega^+)}. \tag{21}$$

Thus, its neglect does not change the qualitative behaviour of the Green's function.

Though the self-energy $\Sigma^{(2)}$ can be expressed in terms of elementary functions, the investigation of the spectral function for the Hubbard model by analytic means is much more complicated due to the interplay of the different terms in equation (9), especially if $\mu \neq 0$. A discussion of the full spectral function by analytic means would become fairly long and less instructive than the presented investigation of the separate contributions. This is mainly due to the fact that the different contributions from the self-energy no longer add in a simple way. For a more detailed discussion see [22]. Here, we prefer to handle the complete spectral function numerically instead.

3. The perturbation result for the spectral density

We will calculate the density of states $\rho^{(2)}(\omega)$ numerically for the cosine dispersion, by a method based on the technique derived in [14] and [22]. Making use of the equations (3) and (4), one finally obtains for $\mu = -0.2$ and $U = 2$ the density of states presented in figure 5.

The infrared behaviour of the exact density of states for the one-dimensional Hubbard model is known: $\rho(\omega) \propto |\omega|^\alpha$, where $\alpha \simeq u$ in the weak-coupling limit [9]. This should produce a dip in the density of states curve at $\omega = 0$, however in figure 5 only sharp features are seen, which do not resemble a logarithmic depression of the density of states we expect. This defect arises as the Umklapp term no longer fits in the geometry of the Fermi surface for $\mu \neq 0$. So, one has to add a constant to $\mathrm{Re}\Sigma$ in order to eliminate this fault. This can be thought as a renormalization of the one-particle energies. Here, the constant has to be chosen in such a way that the particle number is not changed by the interaction, i.e. the

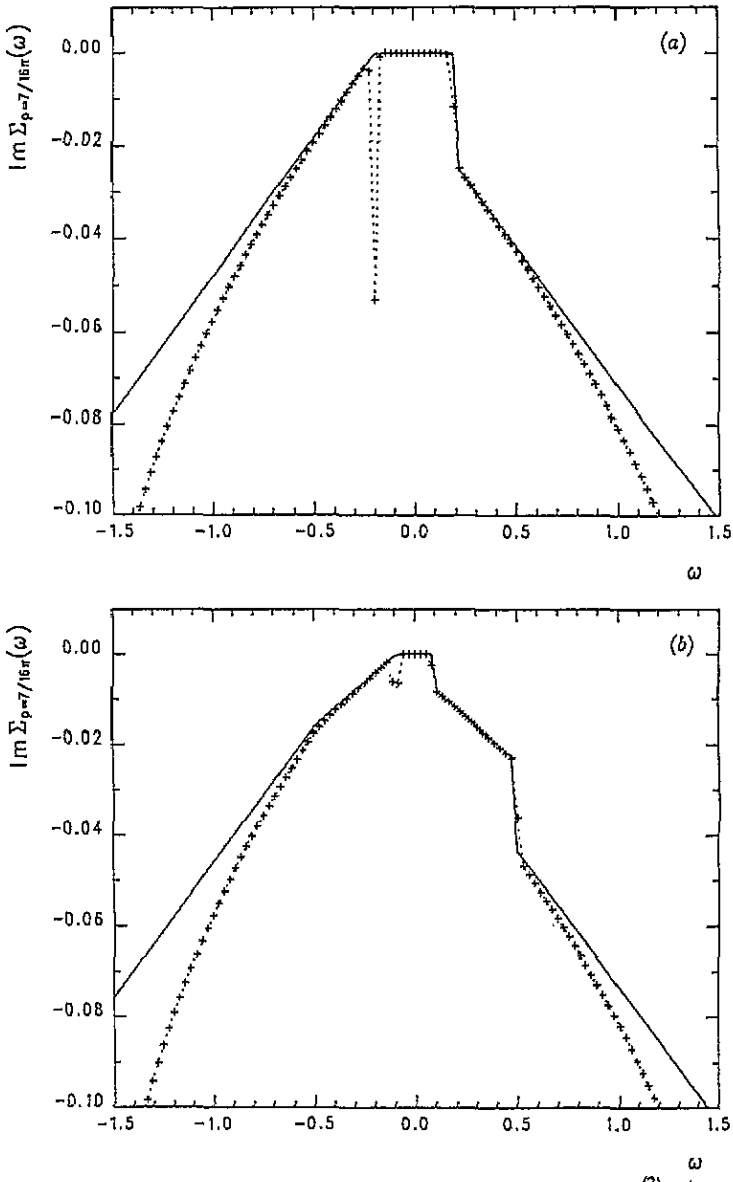

Figure 3. Comparison of the numerical data (crosses, dotted line) for Im $\Sigma_p^{(2)}(\omega^+)$ to the analytic expression (20) (solid line). In both figures we chose $U = 1$, and $p = 7\pi/16$ which corresponds to $\xi_p = -0.20$ for $\mu = 0$ in (a), and to $\xi_p = -0.10$ for $\mu = -0.1$ in (b). The numerical data reproduce very well the typical properties of Im Σ: its linearity for frequencies close to ξ_p and the δ-function contribution due to the Tomonaga process (the δ-function contribution is not shown in the analytic curve).

self-energy. The resulting renormalized density of states is in accordance with Luttinger's theorem [15] and the correct density of states is shown in figure 6.

Though we can only present a numerical result for $\rho(\omega)$ in figure 6, we expect the same logarithmic approximation of the power-law behaviour mentioned above, as it has been derived analytically for the Luttinger processes (equations (17) and (19)). Since both

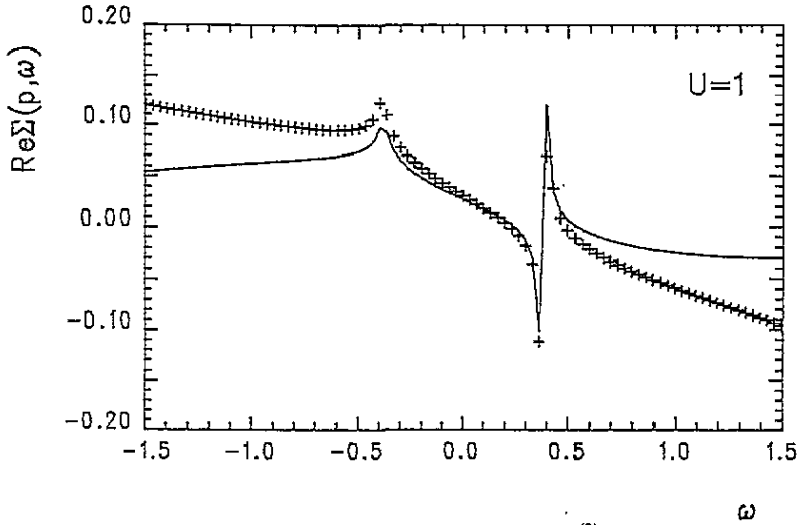

Figure 4. Comparison of the numerical data (crosses) for Re $\Sigma_p^{(2)}(\omega^+)$ to the analytic result (solid line). In this figure we chose $p = 5\pi/8$, $\mu = 0$ which corresponds to $\xi_p = 0.38$.

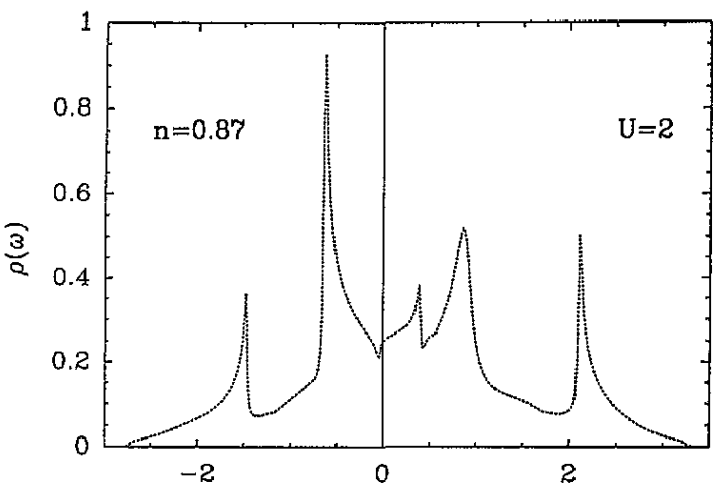

Figure 5. The density of states $\rho(\omega)$, calculated numerically without renormalization. The self-energy has been calculated for $\mu = -0.2$.

Luttinger and backscattering processes contribute equally to the self-energy (9), the critical exponent in equation (17) has to be taken twice. Thus, second-order perturbation theory yields a critical exponent which we estimate to be four times as large as the exact value. With respect to a quantitative agreement, the perturbative result should not be overemphasized.

The weight of the spectral density is also strongly reduced in the vicinity of $\omega = -2\mu$. This second minimum can be easily understood as a consequence of the misfit between Σ^U and Σ^L (8), (9), following the argumentation given in the preceding section, and recalling that most of the weight in the spectral function is centred around $\omega = \xi_p$ in the weak-coupling limit.

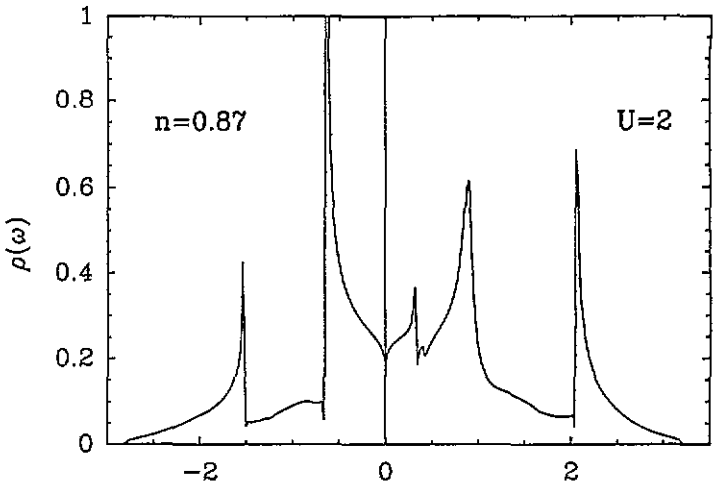

Figure 6. The density of states $\rho(\omega)$, calculated numerically using the renormalization procedure. The self-energy has been calculated for $\mu = -0.2$.

4. Conclusions

We have investigated the perturbative approach to systems of interacting fermions in one dimension. The classification of scattering processes we can use in this case enables us to determine its range of validity and to localize its defects. For the Hubbard model our analysis yields the following results.

For the general case the perturbation results are reliable and can be used to get an insight into the qualitative behaviour of the model. Deviations from Fermi-liquid behaviour can be detected from the numerical data for the self-energy and from the density of states, if one renormalizes the real part of the self-energy correctly in order to keep the particle number constant. Also the separation of spin- and charge-density excitations can be detected easily from the numerical data. However, the insulating property of the Hubbard model cannot be reproduced by perturbation theory.

We would think that in higher dimensions perturbation theory will give qualitatively correct results since in the general case a Fermi-liquid behaviour is expected [4]. This is exactly what this approach would construct. A problem will arise since both the particle number and the shape of the Fermi surface will change, due to the fact that Re $\Sigma_{\vec{p}}(\omega = 0)$ will depend on the Fermi momentum $\vec{p}_f$. One way of circumventing this problem is to include the real part of the self-energy for $\omega = 0$ as an additional part to the kinetic energy and to reach self-consistency by keeping the particle number fixed, as in the one-dimensional case. Only in the many-band case will this lead to complications since the self-energy is certainly not 'band-diagonal'.

The simple perturbation approach will fail to describe the exceptional behaviour of the model when particle–hole symmetry is present. This may occur together when parts of the Fermi surface are nested and deviations from Fermi-liquid behaviour can be expected.

Thus, a naive use of the perturbation expansion for systems of weakly correlated fermions may lead to severe misinterpretations. There are special problems with the Hubbard model, since all scattering processes have the same strength. This is certainly not realistic and would change if one could renormalize its coupling constants as is done in the one-dimensional case.

Acknowledgment

Two of us (BH and VZ) acknowledge financial support from the Alexander von Humboldt Stiftung.

References

[1] Sólyom J 1979 *Adv. Phys.* **28** 201
[2] Haldane F D M 1981 *J. Phys. C: Solid State Phys.* **14** 2585
[3] Luther A 1994 *Phys. Rev.* B **50** 11 446
[4] Castellani C, Di Castro C and Metzner W 1994 *Phys. Rev. Lett.* **72** 316
[5] Neto C and Fradkin E 1995 *Phys. Rev.* B **51** 4084
[6] Rhodes C J and Jacobs R L 1993 *J. Phys.: Condens. Matter* **5** 5649
[7] Lieb E H and Wu F Y 1968 *Phys. Rev. Lett.* **20** 1445
[8] Ogata M and Shiba H 1990 *Phys. Rev.* B **41** 2326
[9] Schulz H J 1990 *Phys. Rev. Lett.* **64** 2831
[10] Frahm H and Kotepin V E 1990 *Phys. Rev.* B **42** 10553; 1991 *Phys. Rev.* B **43** 5653
[11] Kawakami N and Yang S-K 1990 *Phys. Lett.* A **148** 359; 1991 *J. Phys.: Condens. Matter* **3** 5983
[12] Schadschneider A and Zittartz J 1991 *Z Phys.* B **82** 387
[13] Abrikosov A A, Gorkov L P and Dzyaloshinski I E 1964 *Methods of Quantum Field Theory in Statistical Physics* (Englewood Cliffs, NJ: Prentice-Hall)
[14] Zlatić V, Horvatić B, Schliecker G and Schotte K-D 1992 *Phil. Mag.* B **65** 1225
[15] Luttinger J M and Ward J C 1960 *Phys. Rev.* **118** 1417
Luttinger J M 1960 *Phys. Rev.* **119** 1153
[16] Serene J W and Hess D W 1991 *Phys. Rev* B **44** 3391
[17] Schweitzer H and Czycholl G 1991 *Z. Phys.* B **83** 93
[18] Luttinger J M 1963 *J. Math. Phys.* **4** 1154
[19] Emery V J, Luther A and Peschel I 1976 *Phys. Rev.* B **13** 1272
[20] Rozenberg M J, Zhang X Y and Kotliar G 1992 *Phys. Rev. Lett.* **69** 1236
Gros C, Wenzel W, Valenti R, Hülsenbeck G and Stolze J 1994 *Europhys. Lett.* **27** 299
[21] Meden V and Schönhammer K 1992 *Phys. Rev.* B **46** 15753
Schönhammer K and Meden V 1993 *Phys. Rev* B **47** 16205
Voit J 1993 *Phys. Rev.* B **47** 6740
[22] Schliecker G 1994 Spektrale Eigenschaften des Hubbardmodells in niedrigen Dimensionen *Thesis* Freie Universität Berlin